TISSUE ENGINEERING: Part A
Volume 15, Number 8, 2009

DOI: 10.1089/ten.tea.2008.0214

Original Article

The Dose of Growth Factors Influences the Synergistic Effect of Vascular Endothelial Growth Factor on Bone Morphogenetic Protein 4–Induced Ectopic Bone Formation

Guangheng Li, M.D., Ph.D.,[1] Karin Corsi-Payne, Ph.D.,[1] Bo Zheng, M.D.,[1] Arvydas Usas, M.D.,[1] Hairong Peng, M.D., Ph.D.,[2] and Johnny Huard, Ph.D.[1]

Although vascular endothelial growth factor (VEGF) has been shown to act synergistically with bone morphogenetic protein (BMP)2 and BMP4 to promote ectopic endochondral bone formation via cell-based BMP gene therapy, the optimal ratio of VEGF to either of the BMPs required to obtain this beneficial effect remains unclear. In the current study, two cell types (C2C12, NIH/3T3) were retrovirally transduced to express BMP4 only or both BMP4 and VEGF. The resulting groups of cells were tested for their cellular proliferation, *in vitro* mineralization capacity, survival potential, and ability to undergo ectopic bone formation when implanted into a gluteofemoral muscle pocket created in severe combined immunodeficient mice. Results showed that VEGF inhibited the *in vitro* calcification of C2C12 and NIH/3T3 cells transduced to express BMP4. *In vivo*, C2C12 and NIH/3T3 cells expressing BMP4 and VEGF displayed significantly less bone formation than the same cells expressing only BMP4. *In vivo*, our results indicated that, when the ratio of VEGF to BMP4 is high, a detrimental effect on ectopic bone formation is observed; however, when the ratio is kept low and constant over time, the detrimental effect that VEGF has on ectopic bone formation is lost. Our studies revealed that VEGF's synergistic role in BMP4 induced ectopic bone formation is dose and cell-type dependent, which is an important consideration for cell-based gene therapy and tissue engineering for bone healing.

Introduction

Endochondral bone formation begins as a mesenchymal condensation, which then undergoes cartilage formation and cartilage resorption, coupled with blood vessel invasion and ultimately bone formation. Vascular endothelial growth factor (VEGF) is involved in all of the above steps, which are known to occur during embryonic development of long bones and the healing of bone fractures.[1–4] The essential role of VEGF for the survival of chondrocytes during embryogenesis has been shown using a VEGF knockout mouse model.[5] The VEGF knockout mice exhibited massive chondrocyte death at the center of the epiphysis at embryonic day 16.5 (E16.5), suggesting that VEGF may have a direct role in chondrocyte survival.[5] VEGF has also been shown to play an important role in regulating cartilage resorption and blood vessel invasion, because it is believed to be actively responsible for hypertrophic cartilage neovascularization through a paracrine release by hypertrophic chondrocytes, with invading endothelial cells as the target.[6–8] Alternatively, the blocking of VEGF via the systemic administration of a soluble receptor chimeric protein (Flt-(1-3)-IgG) led to a suppression of blood vessel invasion into the growth plate, concomitant with impaired trabecular bone formation and expansion of the hypertrophic chondrocyte zone.[9] Capillary invasion and restoration of the bone growth plate architecture followed removal of the anti-VEGF treatment. Taken together, these findings indicate that VEGF is an essential coordinator of chondrocyte death, chondroclast function, extracellular matrix remodeling, and angiogenesis in the growth plate.[9]

VEGF also plays an important role in osteoblast biology. It has been shown to induce migration, parathyroid hormone–dependent accumulation and an increase in alkaline phosphatase (ALP) in osteoblasts. It is also thought to be an important regulator of osteoblastic differentiation.[10] Osteoblasts express VEGF receptor (VEGFR)-1 and 2 and neuropilin (Nrp),[11,12] and treatment of mice with a soluble, neutralizing VEGFR decreased angiogenesis, bone formation, and callus mineralization in femoral fractures. In other studies, blocking the function of VEGF with an antiangiogenic agent (TNP-470) or when mice lacked the expression of VEGF isoforms VEGF164 and VEGF188 impaired every step

[1]Stem Cell Research Center, Children's Hospital of Pittsburgh, Pittsburgh, Pennsylvania.
[2]Department of Anesthesiology, West Penn Hospital, Pittsburgh, Pennsylvania.

of endochondral bone formation and led to decreased angiogenesis and bone formation.[13,14] Conversely, exogenous VEGF enhanced blood vessel formation, ossification, and new bone (callus) maturation in mouse femur fractures and promoted bony bridging of a rabbit radius segmental gap defect.[12] Therefore, VEGF is an essential growth factor in regulating the process of endochondral bone formation.

Several studies have applied VEGF in combination with bone morphogenetic protein 4 (BMP4) to promote endochondral bone formation. One study demonstrated that a poly- (lactic-co-glycolic acid) scaffold containing combinations of human bone marrow stromal cells and condensed plasmid DNA encoding BMP4 or VEGF elicited greater bone formation than any single factor alone or combination of the other two factors.[15] Our group has previously reported the synergistic effect of VEGF and BMPs on promoting endochondral bone formation by using muscle-derived stem cells (MDSCs).[16,17] In these studies, the MDSCs were retrovirally transduced to express VEGF, BMP2, or BMP4; the resulting cell populations were then combined at different ratios, based on the number of BMP-expressing cells to VEGF-expressing cells, and implanted into a gluteofemoral (GF) skeletal muscle pocket of mice. A ratio of 5:1, which corresponded to the implantation of five BMP4-expressing MDSCs for every VEGF-expressing MDSC, was found to promote bone formation better than the implantation of cells expressing BMP4 only.[16] Although these studies were informative as to the importance of VEGF in promoting endochondral bone formation, they did not take into account the effect that cellular proliferation may have had on the *in vivo* ratio of BMP4 to VEGF. Once the cells expressing BMP4 or VEGF were implanted into the skeletal muscle pocket, they may have proliferated at different rates, and this would change the initial pre-implantation ratio of BMP4 to VEGF.

To determine how the stable ratio of BMP4 to VEGF *in vivo* might affect VEGF's promoting role in endochondral bone formation induced by cell-based gene therapy, we used a cell-mediated double-gene co-expressing approach that kept the ratio of BMP4 to VEGF constant over time. To do so, two easily accessible mouse cell lines were used in the present study. C2C12 cells (mouse myoblasts) and NIH/3T3 cells (mouse fibroblasts) were transduced with a retro*BMP4* virus only or a combination of retro*BMP4* and retro*VEGF* viruses, and their osteogenic potential was compared at different time points *in vitro* and postimplantation *in vivo*.

Materials and Methods

Cell culture

C2C12 cells and NIH/3T3 cells were purchased from the American Type Culture Collection (Manassas, VA). All cells were cultured in Dulbecco's Modified Eagle's Medium (DMEM) supplemented with 10% Fetal Bovine Serum (FBS) and 1% penicillin-streptomycin and incubated at 37°C in humidified air mixed with 5% carbon dioxide (CO_2).

Construction of retroviral vectors expressing lacZ, human BMP4, and VEGF

A retrovirus carrying genes for the nuclear localizing signal and β-galactosidase was produced from a stably transfected cell line known as Tel-6.[18] Retro*BMP4* is an MFG-based retroviral vector containing the human *BMP4* gene plasmid, pCL*BMP4*. Retroviral vectors expressing human VEGF were constructed by cloning the *VEGF165*cDNA (InvivoGen, San Diego, CA) into pCLX, resulting in pCL*VEGF*.[16] The retroviruses expressing *BMP4* and *VEGF* were termed retro*BMP4* and retro*VEGF*, respectively.

Cell transduction using the same concentration of retroBMP4 and retroVEGF

C2C12 cells were seeded at a density of 1.5×10^5 cells per 75-cm^2 flask and were grown to 50% confluence. On the day of transduction, cells were washed twice with sterile Phosphate Buffered Saline (PBS) and incubated with a mixture of 10 mL of retro*BMP4* viral suspension (1×10^6–5×10^6 colony forming units (cfu)/mL), 10 mL of DMEM supplemented with 10% FBS, and hexadimethrine bromide (8 μg/mL). Transduction was carried out at 37°C in 5% CO_2 for a total of 48 h, and the viral suspension was replaced at 16 h and 32 h. The culture medium from C2C12 cells transduced with retro*BMP4* (C2C12-B) was collected after 48 h, centrifuged for 5 min at 2000 rpm at 4°C to remove cellular debris, and used to perform a BMP4 bioassay.

Cells were then transduced a second time with retro*VEGF*. The same protocol as described above was used for this second transduction. C2C12-B cells were cultured in retro*VEGF* viral suspension (1×10^6–5×10^6 cfu/mL) for a total of 48 h, with medium being changed every 16 h, as described above. The culture medium from C212-B cells transduced with retro*VEGF* (C2C12-B-V) was collected after 48 h, centrifuged for 5 min at 2000 rpm at 4°C, and used to perform a VEGF assay (Enzyme-Linked ImmunoSorbent Assay (ELISA)). C2C12 cells were also transduced solely with a retro*VEGF* to create the C2C12-V cells, following the same protocols detailed above. NIH/3T3 cells were transduced and analyzed using the same methods as the C2C12 cells. NIH/3T3 cells transduced with retro*BMP4* were termed 3T3-B, and these 3T3-B cells were then transduced with retro*VEGF* and named 3T3-B-V. Exclusively for the C2C12-B-V cell group, they were transduced a third time with a retro*LacZ* virus according to the protocol described above, which yielded the C2C12-B-V-L cell group for the *in vivo* experiments.

Cell transduction with retroBMP4 and various concentrations of retroVEGF

Retro*VEGF* suspension used in the previous section was diluted 0, 5, and 50-fold, and used to transduce C2C12-B and 3T3-B cells according to the protocol described above. This resulted in the following cell groups: C2C12-B-V50 (retro*VEGF* diluted by a factor of 50), C2C12-B-V5 (retro*VEGF* diluted by a factor of 5), and C2C12-B-V0 (undiluted retro*VEGF*). For the 3T3 cells, the new populations were also named according to the retro*VEGF* dilution (3T3-B-V50, 3T3-B-V5, 3T3-B-V0).

BMP4 bioassay and quantification of VEGF production using untransduced and transduced cells

A previously described BMP4 bioassay[19] was used to determine the level of bioactive BMP4 secreted by the transduced cells. ELISA kits (Human VEGF ELISA Kit, R&D Systems, Minneapolis, MN) were used to quantify the amount of VEGF being secreted by the transduced cells.

Cell proliferation assay

C2C12, C2C12-V, C2C12-B, and C2C12-B-V were assayed for their cell proliferation rate in cell culture medium (DMEM with 1% FBS). A 200-μL cell suspension of C2C12, C2C12-V, C2C12-B, and C2C12-B-V cells was plated in triplicate on the 96-well plates (6.25×10^3 cells/well). Cells were cultured in the 96-well plates for 2 days, after which 20 μL of CellTiter 96 AQ_{UEOUS} One Reagent (Promega, Madison, WI) was added to each well. The plate was subsequently incubated in 5% CO_2 at 37°C for 2.5 h, and the absorbance was read at 490 nm using a 96-well plate reader. NIH/3T3 cell groups were investigated in the same manner.

Pellet culture

Mineralization assay. The four transduced cell groups (C2C12-B, C2C12-B-V, 3T3-B, 3T3-B-V) were cultured as pellets to evaluate calcification *in vitro*. Briefly, 2.5×10^5 cells were centrifuged at 500 *g* in 15-mL polypropylene conical tubes, and the resulting pellets were cultured for up to 4 weeks in osteogenic medium (DMEM supplemented with 10%FBS, 1% penicillin/streptomycin, 10^{-7} M dexamethasone, 50 μg/mL ascorbic-acid-2-phosphate, and 10^{-2}M β-glycerophosphate), which was changed every 2 to 3 days. Samples were harvested on days 7, 14, 21, and 28 and embedded in paraffin block. Pellet sections were stained with von Kossa/eosin staining.

Chondrogenesis assay. 3T3-B and 3T3-B-V cells were made into pellets as described above and cultured in chondrogenic medium (Lonza Group Ltd, Basel, Switzerland). Samples were harvested on days 21 and 28 and embedded in a paraffin block, and the pellet sections were stained with Alcian blue/nuclear fast red.

Terminal deoxynucleotidyl transferase 2′-deoxyuridine 5′-triphosphate nick end labeling assay. The deparaffinized chondrogenic pellet sections of 3T3-B and 3T3-B-V were digested with proteinase K following the protocol provided by the manufacturer (ApopTag Plus Peroxidase *In Situ* Apoptosis Detection Kit, Chemicon, Temecula, CA). The terminal deoxynucleotidyl transferase 2′-deoxyuridine 5′-triphosphate nick end labeling (TUNEL) stain was visualized using a substrate system that stained purple (VIP Substrate Kit, Vector Laboratories, Burlingame, CA). After staining, the sections were examined under the microscope, and positive cells found in the center area of the pellets were quantified.

Western blot analysis for the expression of Nrp-1 and hypoxia-inducible factor 1 subunit alpha in 3T3 cells

3T3, 3T3-B, and 3T3-B-V cell lysates in sample buffer (2-mercaptoethanol and Laemmli sample buffer, Bio-Rad Laboratories, Hercules, CA) were collected, incubated in boiling water for 5 min, and centrifuged, and the supernatant was stored at 4°C. Samples were resolved on 10% sodium dodecyl sulfate–polyacrylamide gels and then transferred to pure nitrocellulose membranes (Bio-Rad Laboratories). The membranes were treated as detailed in the manufacturer's protocol (Vectastain ABC-AmP, Vector Laboratories). Anti-nrp-1 (PC343T, 1:100, Calbiochem, San Diego, CA) and hypoxia-inducible factor 1 subunit alpha (HIF-1α) antibody (38-9800, 1:100, Zymed, South San Francisco, CA) were used for this experiment.

Viability assay of 3T3, 3T3-B, and 3T3-B-V cells

Three groups of 3T3 cells were plated in triplicate on the 96-well plates (1.25×10^4 cells/well). Cells were cultured in DMEM supplemented with 1% FBS and 100 μm or 400 μm hydrogen peroxide (H_2O_2) in the 96-well plates for 2 days. After 2 days, 20 μL of CellTiter 96 AQ_{UEOUS} One Reagent (Promega, Madison, WI) was added to each well; the plate was subsequently incubated for 2.5 h, and the absorbance was read at 490 nm using a 96-well plate reader.

Preparation of gelatin sponge implants

A 100-μL cell suspension containing 2×10^5 cells (for each group of C2C12 and NIH/3T3 cells) was seeded on the surface of a 6- × 6-mm piece of sterile gelatin sponge (Gelfoam; Pharmacia & Upjohn Co, Kalamazoo, MI). After the Gelfoam absorbed the cell suspension, 3 mL of DMEM supplemented with 10% FBS was added to each well, and the implants were incubated overnight. The following day, the seeded Gelfoam scaffolds were implanted into the skeletal muscle pocket of the gluteofemoral muscles of severe combined immunodeficient mice. The mice were sacrificed at 7, 10, 14, 20, 27, and 35 days after cell implantation. All animal experiments were conducted with the approval of the Animal Research and Care Committee of the Children's Hospital of Pittsburgh.

Radiographic and histological analyses

Ectopic bone formation was monitored using X-ray examination of the mice at day 28 postimplantation (Model MX-20, Faxitron X-ray Corporation, Lincolnshire, IL). To visualize mineralized matrix deposition and bone volume analysis *in vitro* and *in vivo*, a micro computed tomography (microCT) imaging system (vivaCT40; Scanco Medical, Bassersdorf, Switzerland) was used to scan all of the osteogenic pellets and *in vivo* samples. Tissue samples were obtained at sacrifice, treated with CRYO-GEL Embedding Medium (Cancer Diagnostics, Inc, Birmingham, MI), rapidly frozen in liquid nitrogen precooled 2-methylbutane (Sigma, St. Louis, MO), and stored at −80°C. Frozen sections were stained as detailed below.

Alcian blue/eosin staining

A 1% Alcian blue solution was made with 3% acetic acid. Frozen sections were fixed in 10% neutral buffered formalin for 10 min and rinsed in distilled water. Slides were placed in 3% acetic acid for 3 min and then transferred into the Alcian blue solution for 30 min, after which they were rinsed in running tap water for 1 min and counterstained with eosin.

Von Kossa/eosin staining

Frozen sections were fixed in 10% neutral buffered formalin for 10 min, followed by 3 rinses in distilled water. The slides were then stained in 2% silver nitrate solution in the dark for 15 min, rinsed three times in distilled water, and exposed to light for 15 to 30 min until appropriate stain development was achieved, after which the sections were counterstained with eosin.

Human BMP4 and VEGF immunostaining and hematoxylin staining

The sections were processed for human BMP4 immunostaining as suggested in the manufacturer's protocol (Vectastain Elite ABC kit, Dab Substrate Kit for Peroxidase; Vector Laboratories). Human BMP4 antibody (1:100 dilution, AF757; R&D Systems) and human VEGF antibody (1:100 dilution, AB-293NA; R&D Systems) were used for the immunostaining. These sections were counterstained with hematoxylin.

Quantitative measurement of newly formed cartilage, bone, and the density of human BMP4 and VEGF staining

Full views of histological sections were obtained using microscopy, and various measurements were obtained with Northern Eclipse imaging software (Empix Imaging Inc., Mississauga, Canada). A measurement of the cartilage formation was obtained by analyzing the blue area, which indicated a positive reaction with Alcian blue. A measurement of bone formation was obtained by analyzing the black area, which indicated a positive reaction to von Kossa staining. A measurement of the density of the human BMP4 and VEGF staining was obtained using Northern Eclipse software to analyze the level of brown color, which indicated the positive expression of human BMP4 and VEGF (i.e., a positive result after treatment with the Dab Substrate Kit for Peroxidase).

Immunostaining for lacZ and CD31 in tissue sections of C2C12-B-V-L cells

Tissue sections were fixed in aectone:methanol (1:1) at room temperature for 5 min and then blocked with 7.5% donkey serum and 7.5% goat serum for 30 min. CD31 antibody (1:200 dilution, BD 553370) and lacZ antibody (1:200 dilution, Abcam) were added to the tissue sections for 3 h at room temperature. Sections were washed in PBS three times for 5 min. Secondary antibodies, goat anti-rat 555 (1:300 dilution) and donkey anti-rat 488 (1:300 dilution), were added to sections for 1 h at-room temperature. 4′,6-diamidino-2-phenylindole (1:1000 dilution) was added to sections for 5 min. Sections were washed in PBS three times and examined under a fluorescence microscope.

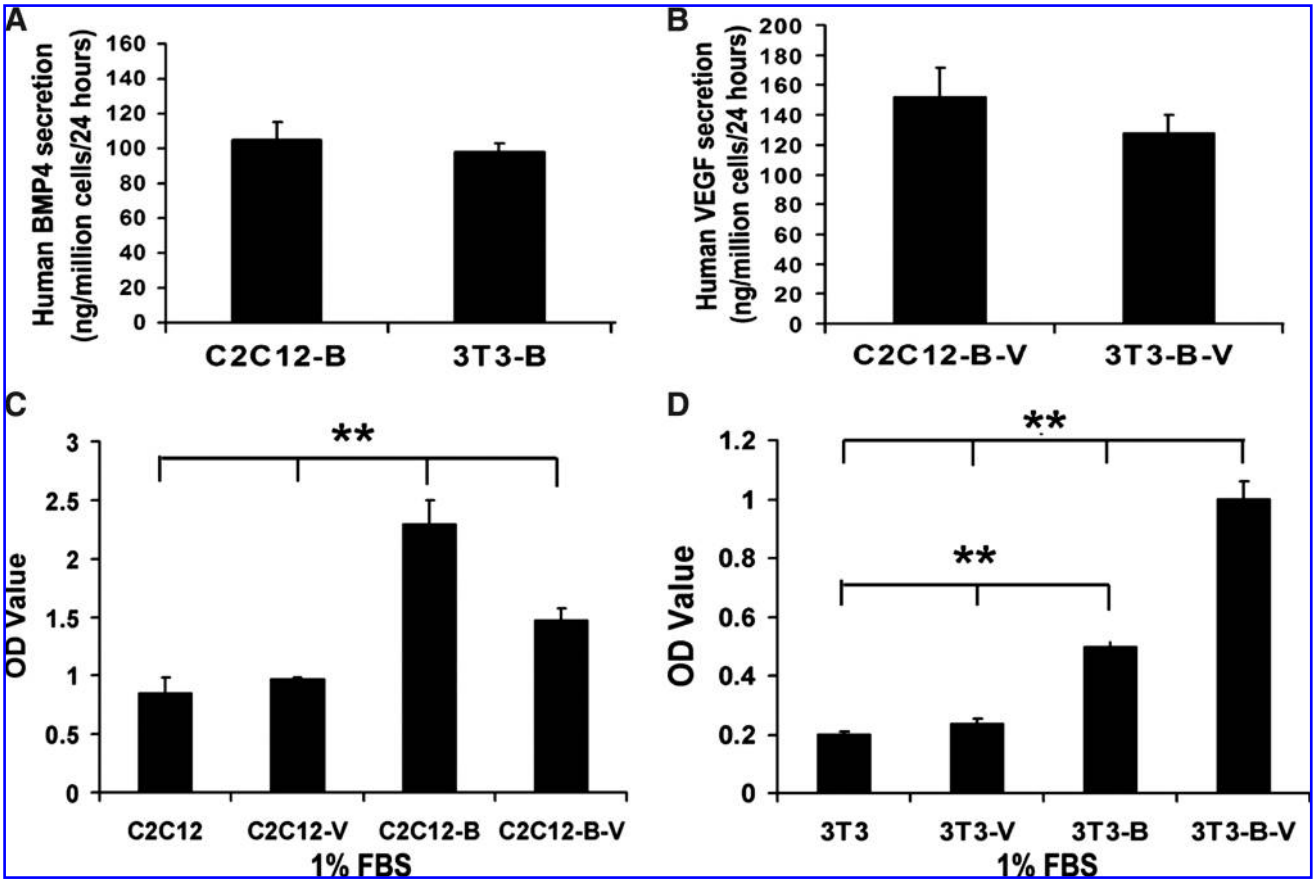

FIG. 1. Growth factors secretion and proliferation rate of genetically engineered cells. (**A**) Amount of recombinant human bone morphogenetic protein 4 (rhBMP4) secreted by C2C12-B and 3T3-B into the culture medium. (**B**) Amount of recombinant human vascular endothelial growth factor (rhVEGF) secreted by C2C12-B-V and 3T3-B-V into the culture medium. (**C, D**) Proliferation of the different populations of (**C**) C2C12 and (**D**) 3T3 cells before and after transduction with retroVEGF, retroBMP4, or both. $^{**}P < 0.01$ indicates a significant difference between (**C**) C2C12-B and all other C2C12 groups, and between (**D**) the 3T3 groups.

Statistical analysis

Data are reported as means ± standard deviations and analyzed using two-way analysis of variance with Tukey's *post hoc* test.

Results

Expression of human BMP4 and VEGF from transduced C2C12 and NIH/3T3 cells

The two types of cells used in this study were both able to synthesize, process, and secrete active recombinant human (rh) BMP4 after transduction with retro*BMP4*. The amount of secreted rhBMP4 reached 105 ± 10 ng/million cells per 24 h in C2C12 cells and 98 ± 5 ng/million cells per 24 h in NIH/3T3 cells (Fig. 1A). The two types of BMP4-expressing cells transduced with retro*VEGF* secreted rhVEGF at a level of 152 ± 20 ng/million cells per 24 h in C2C12 cells and 128 ± 12 ng/million cells per 24 h in NIH/3T3 cells (Fig. 1B). In terms of β-galactosidase gene (LacZ) transduction efficiency, 75% of the C2C12-B-V cells were LacZ positive.

Differential effects of BMP4 and VEGF on the proliferation rate of C2C12 and NIH/3T3 cells

C2C12-V showed a proliferation potential similar to that of the non-transduced C2C12 cells (Fig. 1C). When the C2C12 cells were transduced with retro*BMP4 (C2C12-B)*, their

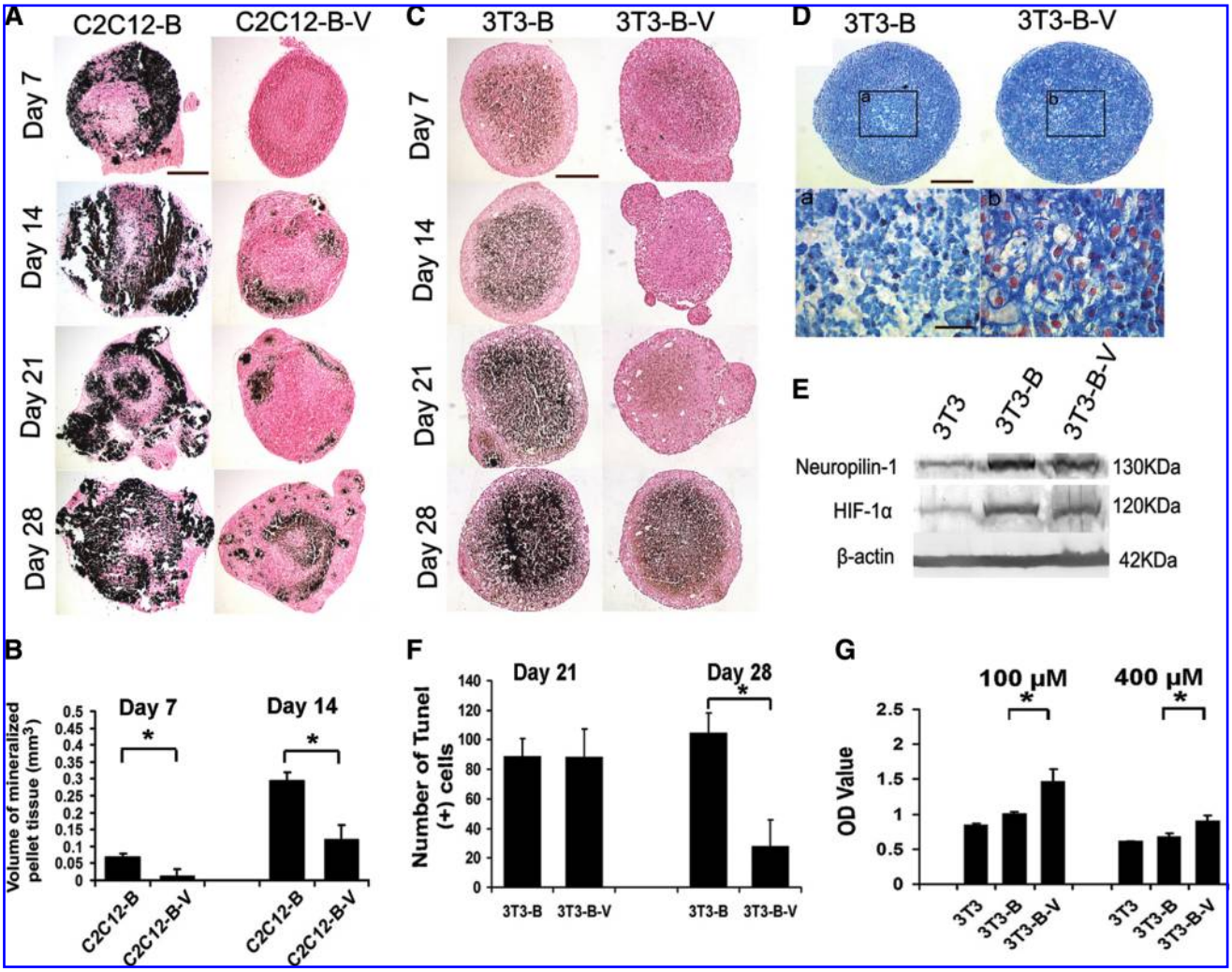

FIG. 2. Mineralization potential and chondrogenic differentiation of C2C12 and NIH/3T3 *in vitro*. With von Kossa/eosin staining, the calcified tissue is stained black and surrounding tissue is stained red. (**A**) C2C12-B-V cell pellets displayed less mineralization than the C2C12-B cells at different time points when cultured in osteogenic medium (scale bar represents 250 μm). (**B**) Micro computed tomography analysis showed that C2C12-B pellets had more mineralized tissue than C2C12-B-V pellets at days 7 and 14 (*$p < 0.05$). (**C**) The 3T3-B-V cell pellets also showed less mineralization than 3T3-B cells (scale bar represents 250 μm). (**D**) With Alcian blue staining, cells in the 3T3-B-V group showed more cells with normal morphology than the 3T3-B group (scale bar represents 50 μm). (**E**) Western blot analysis revealed a differential expression of neuropilin-1 (Nrp1) and hypoxia-inducible factor 1 subunit alpha (HIF-1α) in three 3T3 cell groups. (**F**) Terminal deoxynucleotidyl transferase 2′-deoxyuridine 5′-triphosphate nick end labeling staining of chondrogenic pellets showed less apoptosis in the 3T3-B-V pellets than the 3T3-B pellets at day 28 (*$p < 0.05$), whereas no difference was observed at day 21. (**G**). Oxidative stress analysis showed that 3T3-B-V cells displayed better survival than 3T3-B cells when cultured with 100 μM and 400 μM of hydrogen peroxide (*$p < 0.05$).

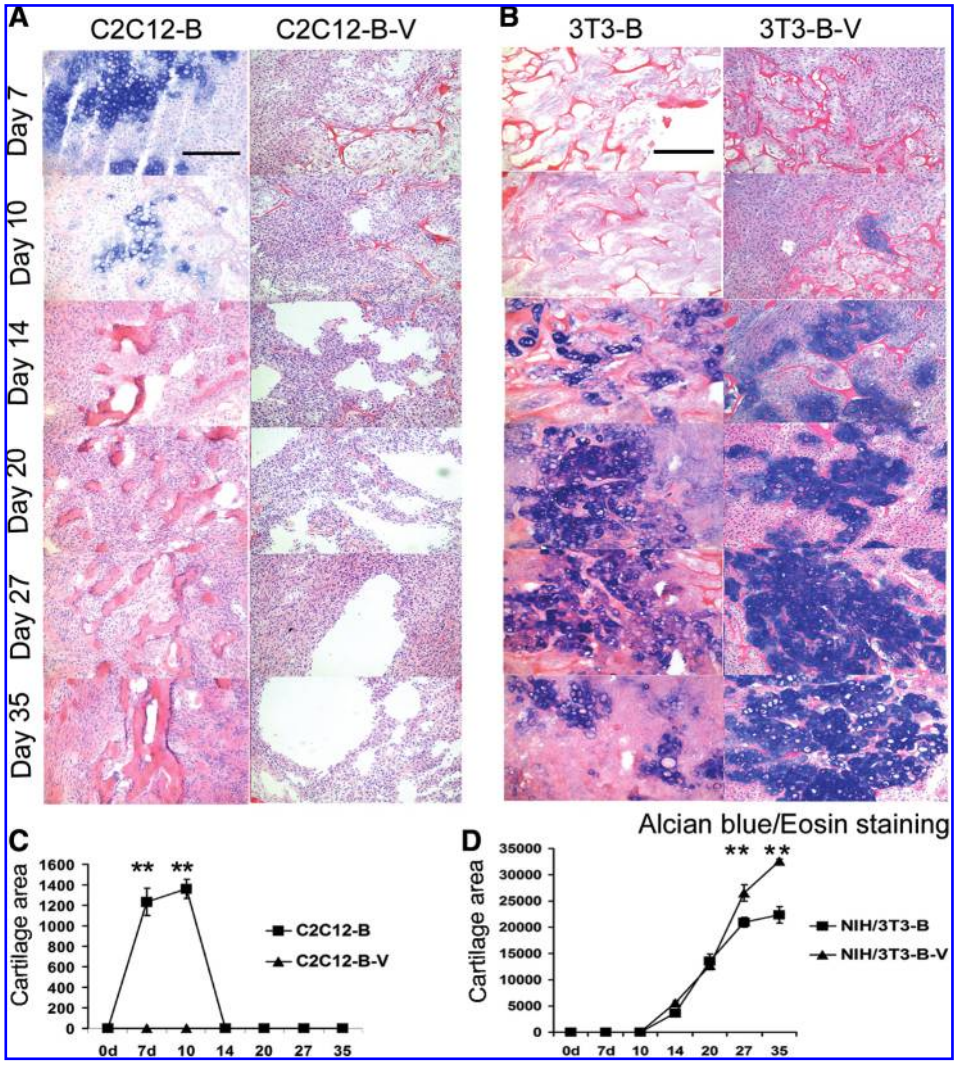

FIG. 3. Characterization of the cartilaginous phase during endochondral bone formation. Alcian blue/eosin staining revealed cartilage tissue, as evidenced by the blue color; the surrounding soft tissue is seen as red. (**A, C**) Cartilage tissue in C2C12-B started to form at day 7, lasted 3 to 7 days, and was resorbed by day 14. C2C12-B-V cells did not have any indication of cartilage formation at any time points examined. This was also confirmed via the quantification of the cartilage area (in pixels) in the three groups (**$p < 0.01$ at days 7 and 10). (**B, D**) The two 3T3 cell groups showed a similar pattern of cartilage formation at the early time points (days 14–20). At days 27 and 35, the 3T3-B-V cell group demonstrated significantly more cartilage formation than the 3T3-B cell groups. The quantification of cartilage area (in pixels) in the three cell groups further confirms this (**$p < 0.01$ at days 27 and 35) (scale bars represent 100 μm).

proliferation potential was significantly greater than that of the C2C12 and C2C12-V cells ($p < 0.01$) (Fig. 1C). However, C2C12-B-V cells displayed significantly poorer proliferation potential than the C2C12-B cells ($p < 0.01$) (Fig. 1C).

3T3 cells and 3T3-V cells displayed similar proliferation rates (Fig. 1D). 3T3-B demonstrated a significantly greater proliferation rate than the 3T3 and 3T3-V cell groups ($p < 0.01$) (Fig. 1D). Transducing these cells to express *BMP4* and *VEGF* (3T3-B-V) led to a significantly greater proliferation rate than that of all other 3T3 cell groups ($p < 0.01$) (Fig. 1D).

Pellet culture

In the *in vitro* mineralization assay, C2C12-B and 3T3-B cell pellets directly calcified without going through a chondrogenic phase when cultured in the osteogenic medium. The C2C12-B-V and 3T3-B-V cell groups showed less calcification than the corresponding C2C12-B and 3T3-B cell groups at different time points (days 7, 14, 21, and 28) (Fig. 2A, C). MicroCT analysis showed that C2C12-B-V pellets displayed significantly less calcified tissue than C2C12-B cell pellets at days 7 and 14 of culture ($p < 0.05$) (Fig. 2B). Results of Alcian blue staining showed that the 3T3-B-V cells exhibited more cells with normal morphology in the center of the pellet than was seen with the 3T3-B cells (Fig. 2D). Western blot analysis showed that the 3T3-B and 3T3-B-V cells expressed similar levels of Nrp-1 and HIF-1α and that both expressed higher levels than the nontransduced 3T3 cells (Fig. 2E). TUNEL staining revealed that pellets made with 3T3-B-V cells had significantly less apoptotic cells than 3T3-B pellets at day 28 of culture ($p < 0.05$) (Fig. 2F).

Survival analysis of different groups of 3T3 cells

3T3-B-V cells showed significantly higher resistance to oxidative stress than 3T3-B cells when cultured in H_2O_2-supplemented DMEM at different concentrations (100 μM and 400 μM) ($p < 0.05$) (Fig. 2G).

*Differential endochondral bone formation displayed by two types of cells transduced with retro*BMP4 *or a combination of retro*BMP4 *and retro*VEGF

C2C12-B cells displayed normal cartilage formation. In the C2C12-B-V group, no cartilage was found at any of the time points tested, yet irregular empty channels were observed (Fig. 3A, C). Although the cartilaginous phase of endochondral bone formation seen with 3T3-B and 3T3-B-V cells was

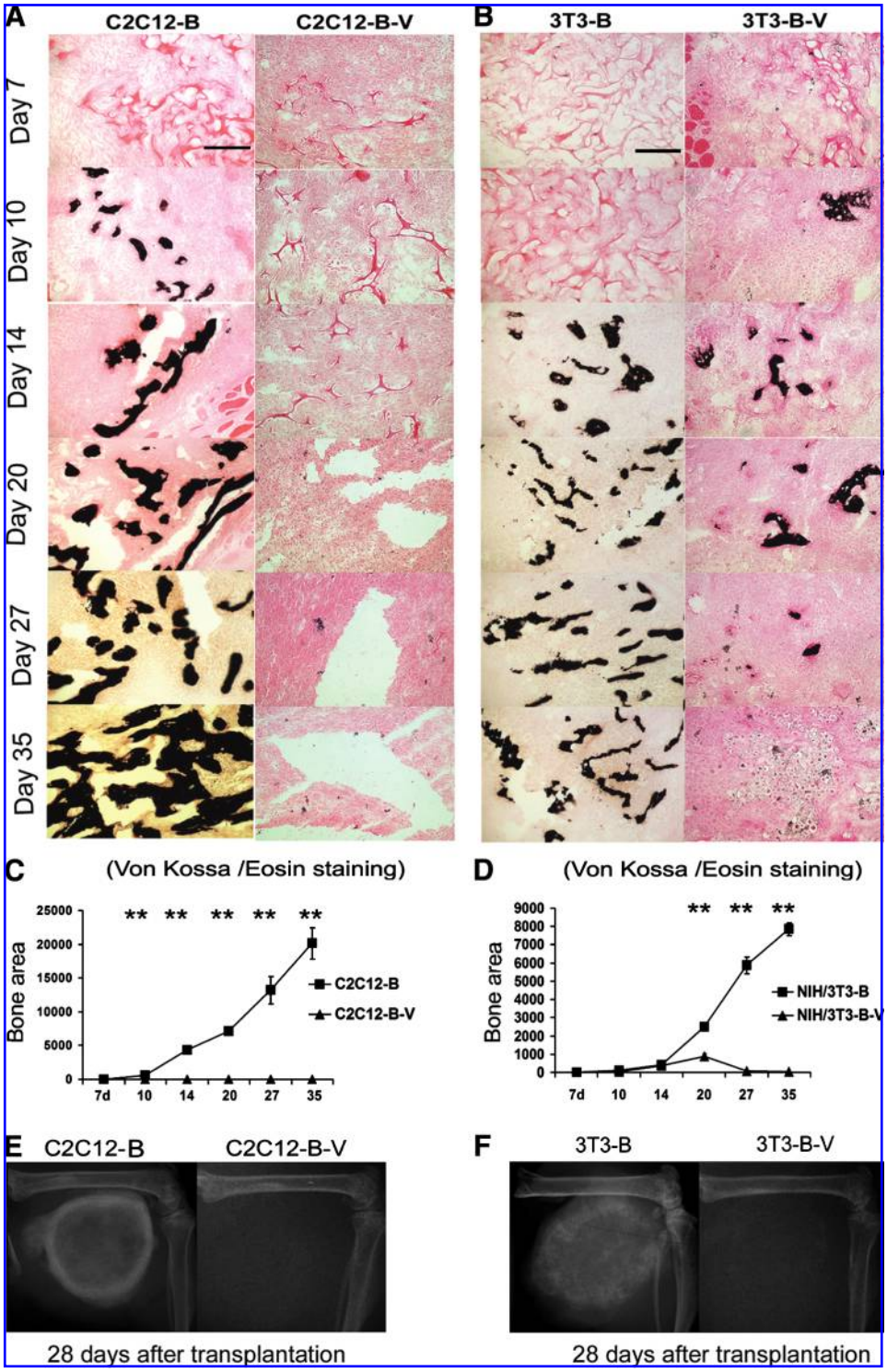

FIG. 4. Characterization of the osteogenic potential of the various cell groups *in vivo*. With von Kossa/eosin staining, the calcified tissue is stained black, and the surrounding soft tissue is stained red. (**A, C**) C2C12-B cells demonstrated bone tissue formation. C2C12-B-V cells did not generate any bone tissue but merely produced a lattice of irregular channels within the soft tissues (scale bars represent 100 μm). The bone area (in pixels) of C2C12-B was significantly larger than that of C2C12-B-V at different time points (**$p < 0.01$ at days 10–35). (**B, D**) 3T3-B cells exhibited a normal pattern of bone formation, whereas 3T3-B-V cells showed poorer bone formation with time (scale bars represent 100 μm). The bone area (in pixels) seen with the 3T3-B cell group was significantly larger than that of the 3T3-B-V cell group (**$p < 0.01$ at days 20–35). (**E**) X-ray analysis at day 28 after implantation showed that the C2C12-B cell group displayed an area of high density in the gluteofemoral muscle pocket of severe combined immunodeficient mice, whereas the C2C12-B-V cells showed no radio-opaque area in the muscle pocket. (**F**) X-ray analysis at day 28 after implantation showed that 3T3-B cells produced an area of high density in the muscle pocket, whereas 3T3-B-V cells exhibited no radio-opaque area in the muscle pocket.

similar at early time points, the 3T3-B-V cells displayed a significantly greater cartilage area at 27 and 35 days post implantation (Fig. 3B, D).

In the case of bone formation, the C2C12-B cell group showed normal bone production (Fig. 4A) (Supplemental Fig. 1, available online at www.liebertonline.com/ten). Implantation of C2C12-B-V cells demonstrated no bone formation at any time points tested, resulting in hemangioma-like structure (Fig. 4A). Among the 3T3 cell groups, the 3T3-B-V cell group displayed a smaller bone area than the 3T3-B cell group at early time points (days 10–14) and almost no bone formation at the later time points (days 27 and 35) (Fig. 4B, D). These observations were also verified using X-ray examination at day 28 postimplantation (Fig. 4E, F). No synergistic effect of VEGF on BMP4-induced bone formation was observed with our primary skeletal muscle cells co-expressing BMP4 and VEGF (Supplemental Fig. 2, available online at www.liebertonline.com/ten).

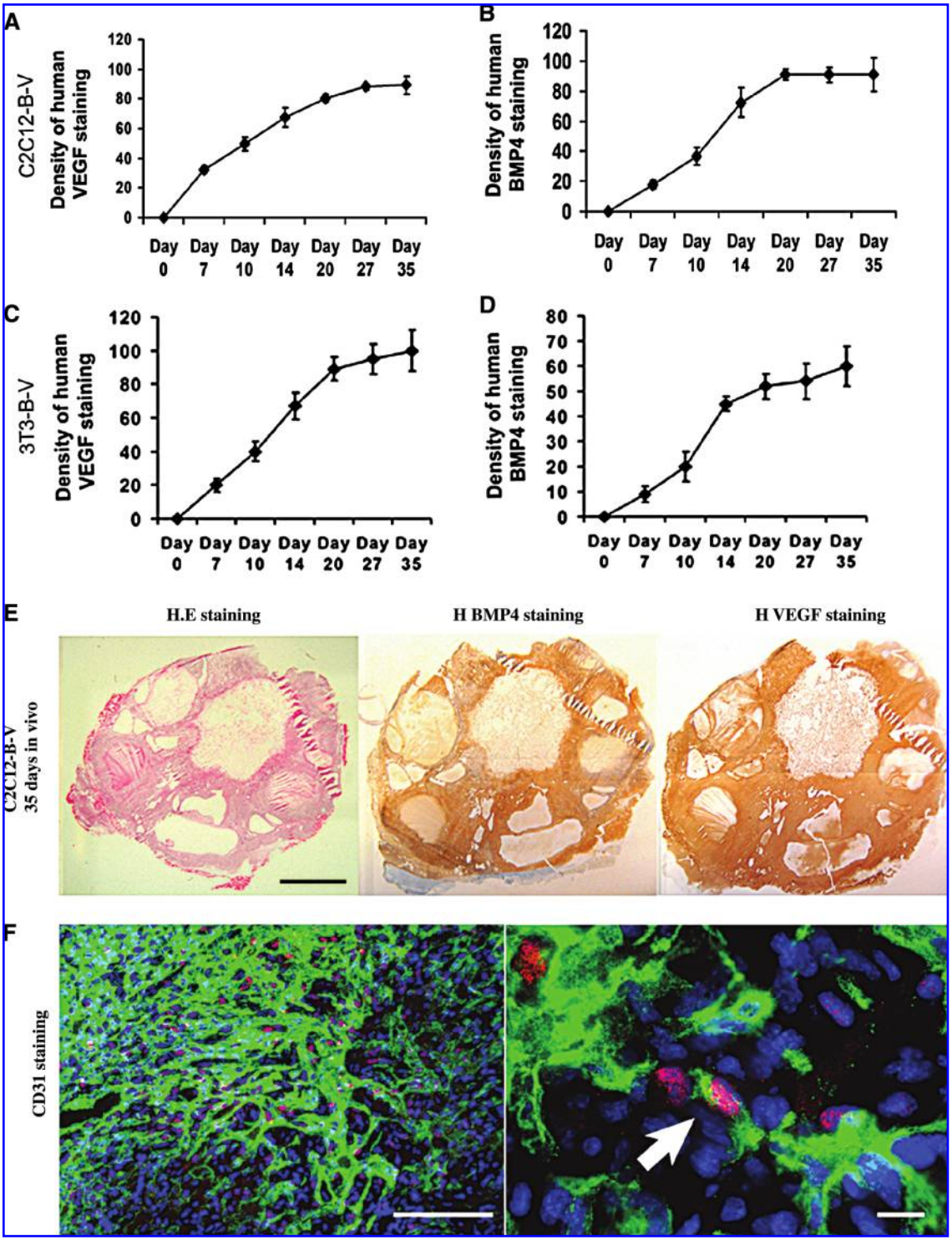

FIG. 5. Expression of human bone morphogenetic protein (BMP)4 and vascular endothelial growth factor (VEGF) *in vivo*. (**A, B**) Staining of the tissue obtained from the C2C12-B-V group at different time points postimplantation showed that human VEGF and BMP4 expression levels increased with time *in vivo*. (**C, D**) 3T3-B-V cells also showed greater human VEGF and BMP4 expression level with time. (**E**) Gross appearance of the *in vivo* tissue sample from the C2C12-B-V group that was stained with hematoxylin and eosin showed a hemangioma-like structure that stained positive for human BMP4 and VEGF (positive = brown color) (scale bar represents 3000 μm). (**F**) The tissue section stained for CD31 and LacZ immunofluorescence (scale bar represents 100 μm) revealed that most cells in the tissue section are CD31 positive (green) and with only a cell positive for both LacZ (red nuclei) and CD31 (green) (arrowhead) (scale bar represents 25 μm) under a higher magnification.

Quantitative measurement of human BMP4 and VEGF immunostaining

Human BMP4 and VEGF immunostaining results of *in vivo* samples (implanted C2C12-B-V and 3T3-B-V cells) at different time points revealed that BMP4 and VEGF expression levels increased with time (Fig. 5A-D).

Results of histological and immunochemical staining

Hematoxylin and eosin staining revealed that C2C12-B-V cells induce a hemangioma-like structure. When these tissues were immunostained with human BMP4 or human VEGF, both proteins were expressed in the tissue sections (Fig. 5E). Although most of the cells in the hemangioma-like structures stained positive with CD31, double staining with lacZ and CD31 indicated that most of the CD31-positive cells were negative for lacZ staining (Fig. 5F).

Co-expression of BMP4 and VEGF at different ratios influence the mineralization potential

C2C12-B and 3T3-B cells secreted different amounts of VEGF after transduction with various concentrations of retro*VEGF* (V50, V5, and V0; Fig 6A, B). The level of secreted VEGF of C2C12-B-V50, C2C12-B-V5, and C2C12-B-V0 reached 16 ± 5 ng/million cells per 24 h, 60 ± 8 ng/million cells per 24 h, and 440 ± 24 ng/million cells per 24 h, respectively. The secreted VEGF level of 3T3-B-V50, 3T3-B-V5, and 3T3-B-V0 reached 4 ± 1 ng/million cells per 24 h, 30 ± 3 ng/million cells per 24 h, and 150 ± 12 ng/million cells per 24 h, respectively. When these various populations of C2C12 and 3T3 cells were implanted *in vivo*, and the mineralized tissue was quantified using microCT, less mineralized potential was observed with greater concentration of secreted VEGF. The cells transduced with nondiluted retro*VEGF* (C2C12-B-V0 and 3T3-B-V0) displayed the lowest amount of mineralized tissue volume, whereas cells transduced with a retro*VEGF* diluted by a factor of 5 and 50 showed significantly greater mineralized tissue volume than the V0 group (Fig. 6C-F).

Discussion

Previous studies have shown that VEGF has a promoting effect on endochondral bone formation induced by BMP4,[16,17] but these studies have relied on the separate delivery of BMP4 and VEGF by transducing cells to express BMP4 or VEGF and then implanting them at certain ratios. Because of this limitation, the possibility cannot be excluded that the BMP4-transduced cells may proliferate at a different rate than the VEGF-transduced cells and consequently influence the initial established ratio of BMP4 to VEGF several days post-implantation. The current study confirmed these differences in proliferation rate by comparing the proliferation rates of untransduced cells with those of cells transduced to express VEGF, BMP4, or both. In the case of C2C12 and NIH/3T3 cells, cells transduced with a retro*BMP4* had a greater proliferation rate than the cells expressing VEGF alone. For this reason, it remains unclear how a ratio of BMP4 to VEGF that remains constant *in vivo* might affect VEGF's promoting role in endochondral bone formation. In this study, we aimed to keep the BMP4:VEGF ratio constant by transducing C2C12 and NIH/3T3 to simultaneously express BMP4 and VEGF. Hence, regardless of the proliferation rate differences, the ratio of BMP4 to VEGF would remain constant over time.

C2C12 cells transduced to express BMP4 have previously been shown to form bone when implanted into the intramuscular pocket of mice.[20] In the present study, when C2C12-B-V cells were analyzed for their ability to form mineralized tissue *in vitro*, it was determined that the co-expression of VEGF inhibited the calcification seen with BMP4-expressing C2C12 cells cultured as pellets in osteogenic medium. This lack of mineralization *in vitro* might explain the subsequent lack of bone formation *in vivo* with the C2C12-B-V cell group, although it is not thought to be the sole explanation, because cell pellets made with C2C12-B-V cells still displayed a certain amount of calcification at days 21 and 28 when cultured in osteogenic medium *in vitro*. Another possibility is that the implanted C2C12-B-V cells may have differentiated into endothelial cells instead of osteoblasts under the synergistic effect of BMP4 and VEGF, although when we followed the fate of the donor cells using LacZ staining, we observed that few donor cells co-expressed the endothelial cell marker CD31, suggesting that the C2C12-B-V cells did not readily differentiate into endothelial cells. The findings observed with C2C12 cells transduced to express BMP4 and VEGF are in accordance with the results from another study that demonstrated that BMP2 could induce vascularization, enhance angiogenesis, and result in vascularized tumor formation.[21] We therefore postulate that implanted C2C12-B-V cells continuously overexpressed VEGF and recruited host cells *in vivo* that consequently participated in the *in vivo* formation of the hemangioma-like structures observed.

Unlike the findings obtained with C2C12-B-V cells, implantation of 3T3-B-V cells led to the formation of tissues filled with a prolonged and more-persistent cartilaginous phase. These findings are in accordance with our previous study, which reported that NIH/3T3 cells have a distinctly greater potential for producing cartilage, both *in vitro* and *in vivo*, when treated with BMP4.[20] The 3T3-B-V cell group produced more cartilage and less bony tissue than the 3T3-B cell group at the different time points (days 27 and 35) after *in vivo* implantation. The mechanism was believed to be different from that of C2C12-B-V cells. The 3T3-B-V cells displayed a greater proliferation potential than the 3T3-B cells, which demonstrated the promoting effect of BMP4 and VEGF on the proliferation of NIH/3T3 cells. In addition, 3T3-B-V cell pellets cultured in chondrogenic medium showed less cell apoptosis than the pellets made with 3T3-B cells. Western blot analysis showed that the co-transduced NIH/3T3 with retro*BMP4* and retro*VEGF* upregulated HIF-1α and the VEGFR Nrp-1. It has been reported that HIF-1α regulates the transcription of a broad range of genes that are involved in a variety of processes such as glucose metabolism, angiogenesis, and cell survival.[22–25] Nrp-1 is a co-receptor membrane-bound to a tyrosine kinase receptor for VEGF that plays a role in angiogenesis, axon guidance, cell survival, migration, and tumor invasion.[11] Our results also indicated that 3T3-B-V cells had a better cell survival rate than 3T3-B and 3T3 cells when they were exposed to oxidative stress. Hence, the greater proliferation and survival potential displayed by 3T3-B-V cells than by 3T3-B cells might explain, at least in part, the observation that more cartilage formation was found in the 3T3-B-V cell group *in vivo*. With regard to the poorer bone production seen in this group than in the 3T3-B group, the

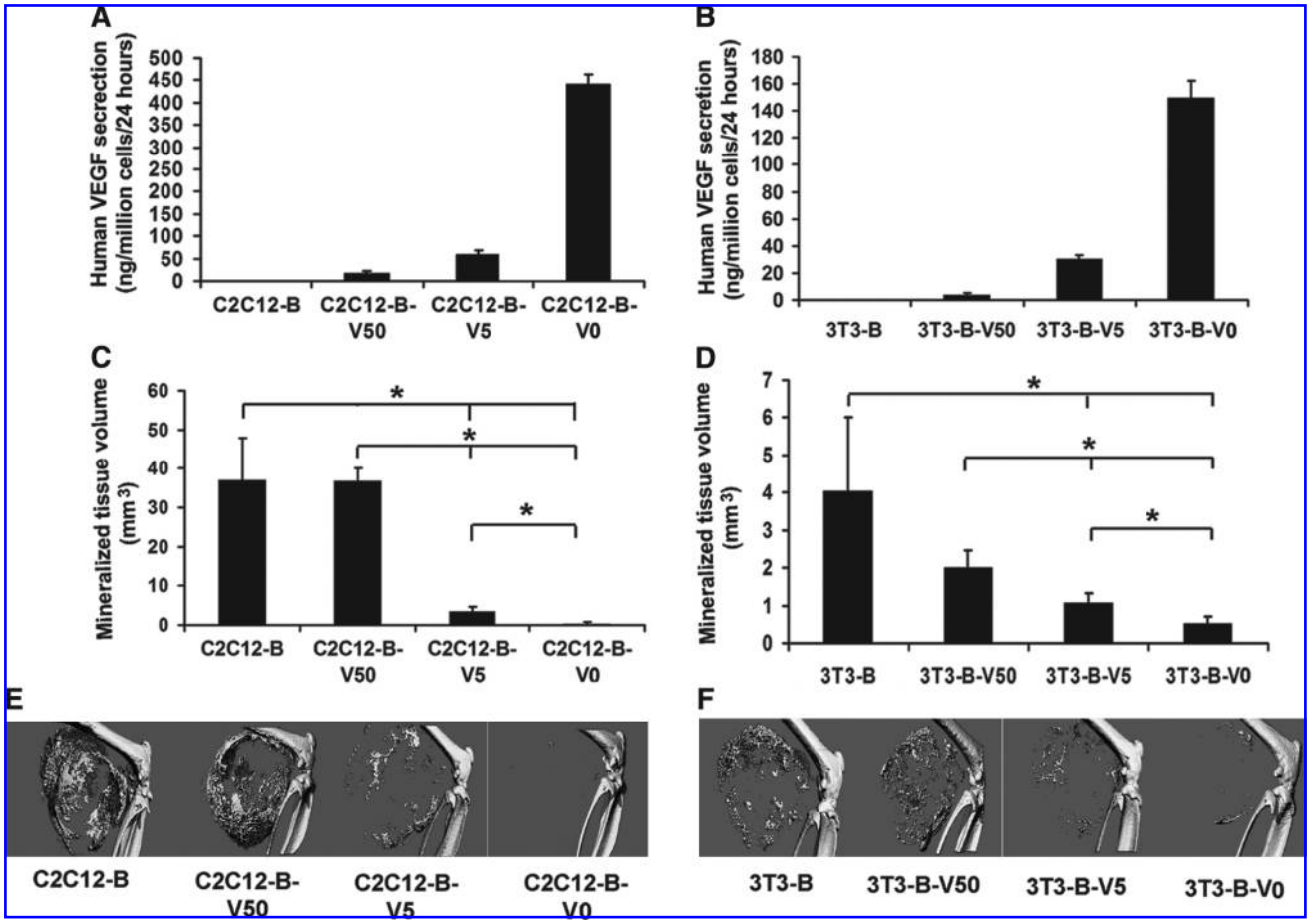

FIG. 6. Mineralization of cells co-expressing bone morphogenetic protein (BMP)4 and vascular endothelial growth factor (VEGF) at various ratios. (**A**) Quantitation of human VEGF secretion in C2C12-B cells and (**B**) 3T3-B cells transduced with retro*VEGF* diluted by a factor of 50 (V50), by a factor of 5 (V5), or undiluted (V0). (**C, D**) Mineralized tissue volume resulting from the *in vivo* ectopic bone production of the four groups of (**C**) C2C12 and (**D**) 3T3 cells. (**C**) Of the C2C12 cell groups, C2C12-B showed the greatest mineralization potential. C2C12-B-V50 showed significantly more mineralized tissue than C2C12-B-V5 or C2C12-B-V0 (*$p < 0.05$). (**D**) Of the 3T3 cell groups, 3T3-B showed the strongest mineralization potential. 3T3-B-V50 showed significantly more mineralized tissue than 3T3-B-V5 or 3T3-B-V0 (*$p < 0.05$). (**E, F**) Micro computed tomography analysis showed the three-dimensional structure of ectopic mineralized tissue in the mouse muscle pockets at day 21 postimplantation and supports the histological findings.

explanation is thought to be that a constant high level of VEGF expression could inhibit the calcification of 3T3-B-V cells *in vivo*, which was supported by the observation that cell pellets made with 3T3-B-V cells have less calcification than those made with 3T3-B cells at different time points (days 7, 14, 21, and 28) when cultured in osteogenic medium *in vitro*.

Transducing C2C12-B and 3T3-B cells with different concentrations of retro*VEGF* further confirmed that co-expression of VEGF and BMP4 lead to impaired mineralized tissue formation, especially with high doses of VEGF. Although diluting the retro*VEGF* by a factor of 5 still impaired bone formation, the dilution by a factor of 50 eliminates the detrimental effect and consequently induces mineralized tissue formation similar to that of the BMP4-only transduced cells. Therefore, these results suggest that co-expression of BMP4 and VEGF in our experimental setting impaired ectopic endochondral bone formation, especially when the ratio of VEGF to BMP4 was high. However, if the ratio of VEGF to BMP4 is kept low and constant, then the detrimental effect on the ectopic bone formation is lost.

In summary, the present study demonstrated that co-expression of VEGF and BMP4 influenced ectopic endochondral bone formation and provided additional knowledge as to the importance of the BMP:VEGF ratio for this process. Although our results indicate that a high ratio of VEGF to BMP4 led to a detrimental effect on bone formation, we have also observed that, if the ratio of VEGF to BMP4 is kept low and constant for a prolonged period of time, detrimental effect of VEGF on bone formation is lost. Therefore, when developing cell-based gene therapies for tissue engineering, it will be important to thoroughly investigate not only the benefits of growth factors, but also their interaction, their respective doses and timing of action, and finally their effect on given cell types.

Acknowledgments

This work was supported in part by a National Institutes of Health grant (1 R01 DE13420-06) to J. Huard. This work was also supported by the William F. and Jean W. Donaldson

Chair at Children's Hospital of Pittsburgh and by the Henry J. Mankin Endowed Chair in Orthopaedic Surgery at the University of Pittsburgh. This investigation was conducted in a facility constructed with support from Research Facilities Improvement Program Grant Number C06 RR-14489 from the National Center for Research Resources, National Institutes of Health.

Disclosure Statement

No competing financial interests exist.

References

1. Ferguson, C., Alpern, E., Miclau, T., and Helms, J.A. Does adult fracture repair recapitulate embryonic skeletal formation? Mech Dev **87,** 57, 1999.
2. Sato, M., Yasui, N., Nakase, T., Kawahata, H., Sugimoto, M., Hirota, S., Kitamura, Y., Nomura, S., and Ochi, T. Expression of bone matrix proteins mRNA during distraction osteogenesis. J Bone Miner Res **13,** 1221, 1998.
3. Vortkamp, A., Pathi, S., Peretti, G.M., Caruso, E.M., Zaleske, D.J., and Tabin, C.J. Recapitulation of signals regulating embryonic bone formation during postnatal growth and in fracture repair. Mech Dev **71,** 65, 1998.
4. Carrington, J.L., and Reddi, A.H. Parallels between development of embryonic and matrix-induced endochondral bone. Bioessays **13,** 403, 1991.
5. Zelzer, E., Mamluk, R., Ferrara, N., Johnson, R.S., Schipani, E., and Olsen, B.R. VEGFA is necessary for chondrocyte survival during bone development. Development **131,** 2161, 2004.
6. Horner, A., Bishop, N.J., Bord, S., Beeton, C., Kelsall, A.W., Coleman, N., and Compston, J.E. Immunolocalisation of vascular endothelial growth factor (VEGF) in human neonatal growth plate cartilage. J Anat **194 (Pt 4),** 519, 1999.
7. Carlevaro, M.F., Cermelli, S., Cancedda, R., and Descalzi Cancedda, F. Vascular endothelial growth factor (VEGF) in cartilage neovascularization and chondrocyte differentiation: auto-paracrine role during endochondral bone formation. J Cell Sci **113 (Pt 1),** 59, 2000.
8. Yee, G., Yu, Y., Walsh, W.R., Lindeman, R., and Poole, M.D. The immunolocalisation of VEGF in the articular cartilage of sheep mandibular condyles. J Craniomaxillofac Surg **31,** 244, 2003.
9. Gerber, H.P., Vu, T.H., Ryan, A.M., Kowalski, J., Werb, Z., and Ferrara, N. VEGF couples hypertrophic cartilage remodeling, ossification and angiogenesis during endochondral bone formation. Nat Med **5,** 623, 1999.
10. Midy, V., and Plouet, J. Vasculotropin/vascular endothelial growth factor induces differentiation in cultured osteoblasts. Biochem Biophys Res Commun **199,** 380, 1994.
11. Harper, J., Gerstenfeld, L.C., and Klagsbrun, M. Neuropilin-1 expression in osteogenic cells: down-regulation during differentiation of osteoblasts into osteocytes. J Cell Biochem **81,** 82, 2001.
12. Street, J., Bao, M., deGuzman, L., Bunting, S., Peale, F.V., Jr., Ferrara, N., Steinmetz, H., Hoeffel, J., Cleland, J.L., Daugherty, A., van Bruggen, N., Redmond, H.P., Carano, R.A., and Filvaroff, E.H. Vascular endothelial growth factor stimulates bone repair by promoting angiogenesis and bone turnover. Proc Natl Acad Sci U S A **99,** 9656, 2002.
13. Mori, S., Yoshikawa, H., Hashimoto, J., Ueda, T., Funai, H., Kato, M., and Takaoka, K. Antiangiogenic agent (TNP-470) inhibition of ectopic bone formation induced by bone morphogenetic protein-2. Bone **22,** 99, 1998.
14. Maes, C., Carmeliet, P., Moermans, K., Stockmans, I., Smets, N., Collen, D., Bouillon, R., and Carmeliet, G. Impaired angiogenesis and endochondral bone formation in mice lacking the vascular endothelial growth factor isoforms VEGF164 and VEGF188. Mech Dev **111,** 61, 2002.
15. Huang, Y.C., Kaigler, D., Rice, K.G., Krebsbach, P.H., and Mooney, D.J. Combined angiogenic and osteogenic factor delivery enhances bone marrow stromal cell-driven bone regeneration. J Bone Miner Res **20,** 848, 2005.
16. Peng, H., Wright, V., Usas, A., Gearhart, B., Shen, H.C., Cummins, J., and Huard, J. Synergistic enhancement of bone formation and healing by stem cell-expressed VEGF and bone morphogenetic protein-4. J Clin Invest **110,** 751, 2002.
17. Peng, H., Usas, A., Olshanski, A., Ho, A.M., Gearhart, B., Cooper, G.M., and Huard, J. VEGF improves, whereas sFlt1 inhibits, BMP2-induced bone formation and bone healing through modulation of angiogenesis. J Bone Miner Res **20,** 2017, 2005.
18. Cosset, F.L., Takeuchi, Y., Battini, J.L., Weiss, R.A., and Collins, M.K. High-titer packaging cells producing recombinant retroviruses resistant to human serum. J Virol **69,** 7430, 1995.
19. Peng, H., Chen, S.T., Wergedal, J.E., Polo, J.M., Yee, J.K., Lau, K.H., and Baylink, D.J. Development of an MFG-based retroviral vector system for secretion of high levels of functionally active human BMP4. Mol Ther **4,** 95, 2001.
20. Li, G., Peng, H., Corsi, K., Usas, A., Olshanski, A., and Huard, J. Differential effect of BMP4 on NIH/3T3 and C2C12 cells: implications for endochondral bone formation. J Bone Miner Res **20,** 1611, 2005.
21. Raida, M., Clement, J.H., Leek, R.D., Ameri, K., Bicknell, R., Niederwieser, D., and Harris, A.L. Bone morphogenetic protein 2 (BMP-2) and induction of tumor angiogenesis. J Cancer Res Clin Oncol **131,** 741, 2005.
22. Zelzer, E., and Olsen, B.R. Multiple roles of vascular endothelial growth factor (VEGF) in skeletal development, growth, and repair. Curr Top Dev Biol **65,** 169, 2005.
23. Lee, J.W., Bae, S.H., Jeong, J.W., Kim, S.H., and Kim, K.W. Hypoxia-inducible factor (HIF-1)alpha: its protein stability and biological functions. Exp Mol Med **36,** 1, 2004.
24. Pugh, C.W., and Ratcliffe, P.J. Regulation of angiogenesis by hypoxia: role of the HIF system. Nat Med **9,** 677, 2003.
25. Semenza, G.L. Targeting HIF-1 for cancer therapy. Nat Rev Cancer **3,** 721, 2003.

Address correspondence to:
Johnny Huard, Ph.D.
Stem Cell Research Center
Children's Hospital of Pittsburgh
4100 Rangos Research Center
3460 Fifth Avenue
Pittsburgh, PA 15213

E-mail: jhuard@pitt.edu

Received: April 11, 2008
Accepted: December 11, 2008
Online Publication Date: February 9, 2009

This article has been cited by:

1. Dr. Yuan Deng, Prof. Huifang Zhou, Dr. Chenxi Yan, Dr. Yefei Wang, Dr. Caiwen Xiao, Prof. Ping Gu, Prof. Xianqun Fan. In vitro osteogenic induction of BMSCs with encapsulated gene modified BMSCs and in vivo implantation for orbital bone repair. *Tissue Engineering Part A* **0**:ja. . [Abstract] [Full Text PDF] [Full Text PDF with Links]
2. Yi Zhou, Xiaoxu Guan, Mengfei Yu, Xinhua Wang, Wenyuan Zhu, Chaowei Wang, Mengliu Yu, Huiming Wang. 2014. Angiogenic/osteogenic response of BMMSCs on bone-derived scaffold: Effect of hypoxia and role of PI3K/Akt-mediated VEGF-VEGFR pathway. *Biotechnology Journal* n/a-n/a. [CrossRef]
3. Laura Kyllönen, Suvi Haimi, Janne Säkkinen, Hannu Kuokkanen, Bettina Mannerström, George K. B. Sándor, Susanna Miettinen. 2013. Exogenously added BMP-6, BMP-7 and VEGF may not enhance the osteogenic differentiation of human adipose stem cells. *Growth Factors* 1-13. [CrossRef]
4. Bo Zheng, Guangheng Li, William C.W. Chen, Bridget M. Deasy, Jonathan B. Pollett, Bin Sun, Lauren Drowley, Burhan Gharaibeh, Arvydas Usas, Bruno Péault, Johnny Huard. 2013. Human myogenic endothelial cells exhibit chondrogenic and osteogenic potentials at the clonal level. *Journal of Orthopaedic Research* **31**:7, 1089-1095. [CrossRef]
5. Jong-Eun Kim, Seong-Su Kang, Kyung-Hee Choi, June-Sung Shim, Chang-Mo Jeong, Sang-Wan Shin, Jung-Bo Huh. 2013. The effect of anodized implants coated with combined rhBMP-2 and recombinant human vascular endothelial growth factors on vertical bone regeneration in the marginal portion of the peri-implant. *Oral Surgery, Oral Medicine, Oral Pathology and Oral Radiology* **115**:6, e24-e31. [CrossRef]
6. Caroline Szpalski, Fabio Sagebin, Marissa Barbaro, Stephen M. Warren. 2013. The influence of environmental factors on bone tissue engineering. *Journal of Biomedical Materials Research Part B: Applied Biomaterials* **101B**:4, 663-675. [CrossRef]
7. Jung-Bo Huh, Mi-Jung Yun, Chang-Mo Jeong, Sang-Wan Shin, Young-Chan Jeon. 2013. Combined effects of rhBMP-2 and rhVEGF coated onto implants on osseointegration: pilot study. *The Journal of Korean Academy of Prosthodontics* **51**:2, 82. [CrossRef]
8. Hongli Sun, Younghun Jung, Yusuke Shiozawa, Russell S. Taichman, Paul H. Krebsbach. 2012. Erythropoietin Modulates the Structure of Bone Morphogenetic Protein 2–Engineered Cranial Bone. *Tissue Engineering Part A* **18**:19-20, 2095-2105. [Abstract] [Full Text HTML] [Full Text PDF] [Full Text PDF with Links] [Supplemental Material]
9. Yi Zhang, Vedavathi Madhu, Abhijit S. Dighe, James N. Irvine, Quanjun Cui. 2012. Osteogenic response of human adipose-derived stem cells to BMP-6, VEGF, and combined VEGF plus BMP-6 in vitro. *Growth Factors* **30**:5, 333-343. [CrossRef]
10. Marcio M. Beloti, Luciana G. Sicchieri, Paulo T. de Oliveira, Adalberto Luiz Rosa. 2012. The Influence of Osteoblast Differentiation Stage on Bone Formation in Autogenously Implanted Cell-Based Poly(Lactide-Co-Glycolide) and Calcium Phosphate Constructs. *Tissue Engineering Part A* **18**:9-10, 999-1005. [Abstract] [Full Text HTML] [Full Text PDF] [Full Text PDF with Links]
11. Björn Behr, Michael Sorkin, Marcus Lehnhardt, Andrea Renda, Michael T. Longaker, Natalina Quarto. 2012. A Comparative Analysis of the Osteogenic Effects of BMP-2, FGF-2, and VEGFA in a Calvarial Defect Model. *Tissue Engineering Part A* **18**:9-10, 1079-1086. [Abstract] [Full Text HTML] [Full Text PDF] [Full Text PDF with Links] [Supplemental Material]
12. Cláudio R. Reis-Filho, Elisângela R. Silva, Adalberto B. Martins, Fernanda F. Pessoa, Paula V.N. Gomes, Mariana S.C. de Araújo, Melissa N. Miziara, José B. Alves. 2012. Demineralised human dentine matrix stimulates the expression of VEGF and accelerates the bone repair in tooth sockets of rats. *Archives of Oral Biology* **57**:5, 469-476. [CrossRef]
13. Chin-Yu Lin, Yu-Han Chang, Chun-Yu Kao, Chia-Hsin Lu, Li-Yu Sung, Tzu-Chen Yen, Kun-Ju Lin, Yu-Chen Hu. 2012. Augmented healing of critical-size calvarial defects by baculovirus-engineered MSCs that persistently express growth factors. *Biomaterials* . [CrossRef]
14. Mandeep S Virk, Osamu Sugiyama, Sang H Park, Sanjiv S Gambhir, Douglas J Adams, Hicham Drissi, Jay R Lieberman. 2011. "Same Day" Ex-vivo Regional Gene Therapy: A Novel Strategy to Enhance Bone Repair. *Molecular Therapy* **19**:5, 960-968. [CrossRef]
15. Tao Luo, Wei Zhang, Bin Shi, Xiangrong Cheng, Yufeng Zhang. 2011. Enhanced bone regeneration around dental implant with bone morphogenetic protein 2 gene and vascular endothelial growth factor protein delivery. *Clinical Oral Implants Research* no-no. [CrossRef]
16. Caiwen Xiao, Huifang Zhou, Guangpeng Liu, Peng Zhang, Yao Fu, Ping Gu, Hongliang Hou, Tingting Tang, Xianqun Fan. 2011. Bone marrow stromal cells with a combined expression of BMP-2 and VEGF-165 enhanced bone regeneration. *Biomedical Materials* **6**:1, 015013. [CrossRef]
17. Yeon Ju Hong, You Won Choi, Ki Bum Myung, Hae Young Choi. 2011. The Immunohistochemical Patterns of Calcification-related Molecules in the Epidermis and Dermis of the Zebrafish (Danio rerio). *Annals of Dermatology* **23**:3, 299. [CrossRef]

18. Quanjun Cui, Edward A. Botchwey. 2010. Emerging Ideas: Treatment of Precollapse Osteonecrosis Using Stem Cells and Growth Factors. *Clinical Orthopaedics and Related Research®* . [CrossRef]
19. Chin-Yu Lin, Yu-Han Chang, Kun-Ju Lin, Tzu-Chen Yen, Ching-Lung Tai, Chi-Yuan Chen, Wen-Hsin Lo, Ing-Tsung Hsiao, Yu-Chen Hu. 2010. The healing of critical-sized femoral segmental bone defects in rabbits using baculovirus-engineered mesenchymal stem cells. *Biomaterials* **31**:12, 3222-3230. [CrossRef]
20. Björn H. Schönmeyr, Marc Soares, Tomer Avraham, Nicholas W. Clavin, Fredrik Gewalli, Babak J. Mehrara. 2010. Vascular Endothelial Growth Factor Inhibits Bone Morphogenetic Protein 2 Expression in Rat Mesenchymal Stem Cells. *Tissue Engineering Part A* **16**:2, 653-662. [Abstract] [Full Text HTML] [Full Text PDF] [Full Text PDF with Links]